Diffusion-controlled growth rate of stepped interfaces

P. Saidi* and J. J. Hoyt
Department of Materials Science and Engineering, McMaster University, Hamilton, Ontario, Canada
(Received 7 January 2015; revised manuscript received 5 May 2015; published 8 July 2015)

For many materials, the structure of crystalline surfaces or solid-solid interphase boundaries is characterized by an array of mobile steps separated by immobile terraces. Despite the prevalence of step-terraced interfaces a theoretical description of the growth rate has not been completely solved. In this work the boundary element method (BEM) has been utilized to numerically compute the concentration profile in a fluid phase in contact with an infinite array of equally spaced surface steps and, under the assumption that step motion is controlled by diffusion through the fluid phase, the growth rate is computed. It is also assumed that a boundary layer exists between the growing surface and a point in the liquid where complete convective mixing occurs. The BEM results are presented for varying step spacing, supersaturation, and boundary layer width. BEM calculations were also used to study the phenomenon of step bunching during crystal growth, and it is found that, in the absence of elastic strain energy, a sufficiently large perturbation in the position of a step from its regular spacing will lead to a step bunching instability. Finally, an approximate analytic solution using a matched asymptotic expansion technique is presented for the case of a stagnant liquid or equivalently a solid-solid stepped interface.

DOI: 10.1103/PhysRevE.92.012404 PACS number(s): 81.10.−h, 68.05.−n, 68.08.−p

I. INTRODUCTION

The mobility of interphase boundaries plays a crucial role in the description of many important processes, from the growth of protein crystals to the heat treatment of alloys. In studying the motion of interfaces, the first level of classification is the distinction between rough and faceted (smooth) interfaces. A rough interface atom attachment to the growing phase occurs readily at any point on the boundary, and rough interfaces are characteristic of solid-liquid interfaces in most metals and alloys. On the other hand faceted interfaces are identified by the presence of immobile terraces separated by steps of roughly atomic height. The description of crystal growth from the vapor as the lateral motion of steps across the surface was first introduced by Frankel [1] and Burton *et al.* [2]. In many alloy systems the interface between a precipitate and the matrix phase can also be described by a series of mobile steps. Thus Aaronson [3] extended the ideas of Burton *et al.* and proposed the so-called ledge mechanism in solid-solid systems. To date, electron microscopy studies, most notably those employing the scanning tunneling microscopy technique [4], confirmed the ledge mechanism in many systems, such as pure Si [5] grown from the vapor and alloying systems [6,7], including steels [8,9] and aluminum alloys [10–16].

The other set of classification in crystal growth theories are diffusion-controlled and/or interface-controlled systems. In the latter case, most theories assume some rate-controlling event to occur on the surface, either as a result of nucleation rates or some process such as adsorption, surface diffusion, or step incorporation [17–19]. Another real possibility is that the solute transfer to the surface may be limited by mass transfer or diffusion through the bulk solution. Despite the importance of diffusion-controlled growth only a limited number of analytic solutions are available. For a planar, rough interface growing in an infinite system the concentration profile can be obtained, and the solution has been utilized in the well-known Mullins and Serkerka instability theory [20,21]. The diffusion-controlled growth of a paraboidal-shaped dendrite has been solved exactly by Ivantsov under the assumption of no capillarity effects. The more general case has been the subject of many theoretical studies and has led to the solvability criterion of velocity selection for dendritic solidification. In many alloy systems platelike precipitates with approximately parabolic tips are observed, and several studies have been conducted to predict the precipitate growth rate from the Ivantsov approach [22–24]. In these studies the relationship between the velocity of the plate tip and supersaturation at a specific tip curvature was predicted. However, the predictions of these models usually show a significant deviation from experimental results [25]. In order to explain this discrepancy several authors examined factors such as anisotropy of the surface energy [26], nonideal solution [27], and, most importantly, inability of a smooth parabola to represent the step-terrace geometry [28].

For faceted interfaces, reliable modeling of the diffusion-controlled ledge mechanism needs a geometry in which mobile steps, as sinks of solute, are positioned at discrete locations along the interphase boundary. This geometry differs from classical models where a uniform flux along the rough interface is assumed. For the case of smooth interfaces, the most general form of the diffusion equation would be the following:

$$D\nabla^2 c - v_K \frac{\partial c}{\partial x} - v_S \frac{\partial c}{\partial y} - v_D \frac{\partial c}{\partial z} = 0, \qquad (1)$$

where v_K, v_S, and v_D are kink, step, and surface velocities, respectively, D is the diffusion coefficient in the matrix phase, and c is the concentration. The solution of Eq. (1) with different simplifying assumptions has been considered in the literature. One of the first models developed by Burton *et al.* [2], known as the BCF model, assumed that steady growth occurs only at energetically favorable kinks. In addition, it was assumed that the relative motion of any sinks such as kinks or steps is negligible when compared with the bulk diffusion fluxes. Therefore they solved $D\nabla^2 c = 0$. Using a set of geometric approximations, and defining the influence region for kinks,

*saidip@mcmaster.ca

steps, and the solidification front, they calculated the interface velocity for systems with equally spaced steps.

When the ledge mechanism is dominant, attachment of the adatom can happen anywhere along the step, which is itself rough. Therefore, in this case, kink formation is unnecessary for the progress of crystal growth. Thus, the term in Eq. (1) that includes the kink velocity can be eliminated. Chernov [29] modified the BCF diffusion model. He made the simplifying assumption that the distance between two successive kinks is so small that one can consider a step as a long sink, and thus the concentration profile is merely dependent on two dimensions perpendicular to the step line. Instead of using an approximate solution by a geometrical division of the domain (as was done by the BCF model), $D\nabla^2 c = 0$ was solved analytically, using a conformal mapping technique, in two dimensions for an infinite and periodic array of steps. However, Chernov used an attachment-limited boundary condition at the steps, rather than a diffusion-controlled condition. In the Chernov approach each step is a source point, and the height of the step is negligible in comparison with the length of the terraces. Besides simple mass transfer limitations, Ohara [30] considered the effect of heat evolution (or absorption) at the crystal interface and derived an equation to account for the simultaneous transfer of heat and mass and concluded that simultaneous heat transfer effects are negligible. In another study by Jones and Trivedi [31], the height of the step was considered explicitly and diffusion control was assumed. The analytic solution was obtained in the limit of a zero Péclet number and is valid for a single isolated step. Atkinson further improved the previous method by calculating the concentration profile in the case of small Péclet numbers by utilizing Fourier transformations, multiple scale analyses, and a singular perturbation method for an isolated step [32], multiple steps [33], and steps close to an external surface [34]. In addition, a finite-difference based diffusional growth model has been used for numerical modeling of the ledge density effects, ledge nucleation kinetics, and the presence of multiple precipitates on solute buildup in the matrix [35–40].

The other phenomenon that can be addressed by solving the diffusion equation is step bunching, which refers to the tendency of a regular spaced step train to become unstable and to form regions of closely spaced steps separated by long terraces. The case of crystals grown from deposition through a vapor phase step bunching has been well studied. In an early treatment of step bunching, Frank explained this phenomenon using an impurity mechanism [41]. A more recent stability analysis [42] has shown that step bunching can occur due to an asymmetric flux to a step arising from the Ehrlich-Schwoebel barrier [43,44].

Crystals grown from the melt the asymmetry in flux and hence step bunching can be provided by flow in the liquid. A far-field liquid flow in the direction of step motion the regular array is stabilized against bunching, whereas flow in the direction counter to the step growth direction acts to destabilize the interface. In several studies Bredikhin and co-workers [45–48] have studied step bunching, and they conclude that, even in the absence of liquid flow, a regular train of steps is inherently unstable due to the interaction between traveling inhomogeneities of step density and diffusion in the solution. The boundary element method (BEM) computations performed here will help address step bunching during diffusion-controlled growth.

The purpose of the present work is to provide numerical and analytic solutions to a growth process of facetted interfaces not yet considered, that is, the diffusion-controlled growth of an infinite train of equally spaced steps. We begin by introducing the boundary element technique for the case where a boundary layer is assumed in the liquid adjacent to the crystal-melt interface and determine the concentration field and growth velocity as a function of step separation and boundary layer width. In addition, we examine the instability of an equally spaced train of arrays by applying a perturbation to a single step and calculating the velocity of the neighboring steps to determine the final stable arrangement of a train of steps. Finally, we present an approximate analytic solution based on a matched asymptotic technique for the case of no boundary layer, which is valid for the case of growing precipitates in alloys.

II. BOUNDARY INTEGRAL FORMULATION

Consider a coordinate system in which the steps are moving at constant velocity in the direction x and the interface as a whole migrates in the y direction. If the step spacing is large, it is reasonable to neglect the velocity in y, and the diffusion equation can be rewritten as

$$D\nabla^2 c + v_x \frac{\partial c}{\partial x} = 0, \tag{2}$$

where v_x is the step velocity, D is the diffusivity in the matrix, liquid or vapor phase, and c is the concentration. The two-dimensional geometry also assumes that the steps are straight. Further we assume that the steps are energetically favorable sites for atom attachment and no surface adsorption at the terraces is allowed.

For convenience we can rewrite Eq. (2) in a dimensionless form by defining a Péclet number $p_x = \frac{v_x h}{D}$ which is scaled by the step height h and a scaled concentration given by the form used by Atkinson: $u = \frac{c-c_0}{c_e-c_0}$. The scaled variables yield the following:

$$\nabla^2 u + p_x \frac{\partial u}{\partial \tilde{x}} = 0. \tag{3}$$

The value of scaled concentration varies between zero for the far field limit and unity for the equilibrium condition. For developing the boundary element formulation, we employed the method used by several authors [28,49–51], which relies on a variable transformation in order to reduce the problem to a Helmholtz equation. The variable transformation has the form $u = \phi e^{-\frac{p_x}{2}\tilde{x}}$. After substituting the final Helmholtz equation obtains as

$$\nabla^2 \phi - \left(\frac{p_x}{2}\right)^2 \phi = 0. \tag{4}$$

The fundamental solution corresponding to Eq. (4) should satisfy the equation

$$\nabla^2 G(\mathbf{r},\mathbf{r}') - \left(\frac{p_x}{2}\right)^2 G(\mathbf{r},\mathbf{r}') = -\delta(\mathbf{r},\mathbf{r}'), \tag{5}$$

where $\mathbf{r}$ and $\mathbf{r}'$ are vectors representing field and boundary points, respectively, δ is the Dirac delta function, and $G(\mathbf{r},\mathbf{r}')$ is

the Green's function for the corresponding Helmholtz equation and is expressible as a function of K_0, the modified Bessel function of the second kind of order zero i.e.:

$$G(\mathbf{r},\mathbf{r}') = \frac{1}{2\pi} K_0\left[\left(\frac{p_x}{2}\right)|\mathbf{r}-\mathbf{r}'|\right], \tag{6}$$

where the Péclet number is defined as a positive quantity.

From Green's theorem, the boundary integral formulation is established:

$$\begin{aligned}\alpha u(\mathbf{r}) &- \int u(\mathbf{r}')\frac{\partial G(\mathbf{r},\mathbf{r}')}{\partial n'} e^{\frac{p_x}{2}(r_x'-r_x)}\, d\Gamma(\mathbf{r}') \\ &+ \frac{p_x}{2}\int G(\mathbf{r},\mathbf{r}')u(\mathbf{r}')\frac{\partial r_x'}{\partial n'} e^{\frac{p_x}{2}(r_x'-r_x)}\, d\Gamma(\mathbf{r}') \\ &= -\int G(\mathbf{r},\mathbf{r}')\frac{\partial u(\mathbf{r}')}{\partial n'} e^{\frac{p_x}{2}(r_x'-r_x)}\, d\Gamma(\mathbf{r}'),\end{aligned} \tag{7}$$

where the parameter α is a constant and its value depends on the location of $\mathbf{r}$. When $\mathbf{r}$ lies inside the domain α takes the value of unity, and when $\mathbf{r}$ lies on a smooth boundary α takes the value $\frac{1}{2}$. In the above equation $\frac{\partial}{\partial n'}$ is the directional derivative of the corresponding function in the direction of the outward pointing normal n' to the surface element $d\Gamma$.The derivative of the fundamental solution appearing in the first integral is

$$\frac{\partial G}{\partial n'} = \frac{p_x}{4\pi} K_1\left(\frac{p_x}{2}|\mathbf{r}-\mathbf{r}'|\right)\frac{(\mathbf{r}-\mathbf{r}')\cdot\mathbf{n}'}{|\mathbf{r}-\mathbf{r}'|}, \tag{8}$$

where K_1 is the modified Bessel function of the second kind of order one.

For boundary integral implementation we follow the procedure explained in detail in Ref. [52] and used in several studies [49,51]. Equation (7) can be rewritten as

$$\alpha u + \int_\Gamma u q^*\, d\Gamma - \int_\Gamma q u^*\, d\Gamma = 0, \tag{9}$$

where we have taken q^* as the coefficients of u and u^* is the coefficients of $q = \frac{\partial u(\mathbf{r}')}{\partial n'}$. The boundary Γ is discretized into N straight line segments where u_j and q_j are respectively approximated as constants, such that they can be removed from the integrals. This yields

$$\frac{1}{2}u_i + \sum_{j=1}^{N}\left(\int_\Gamma q^*\, d\Gamma\right)u_j - \sum_{j=1}^{N}\left(\int_\Gamma u^*\, d\Gamma\right)q_j = 0. \tag{10}$$

After integration the whole set of equations can be expressed in matrix form as

$$[\mathbf{A}]\{\mathbf{Y}\} = [\mathbf{F}], \tag{11}$$

where $\mathbf{Y}$ is the vector of unknowns u or q. For each case the total number of unknowns should be equal to the number of the possible equations for the whole domain. Therefore, we can find the value of scaled concentration and flux for every element on the boundary of the domain. In a postprocessing step one can calculate the concentration at any point in the interior from the known boundary terms.

It is common to employ numerical methods such as Gaussian quadrature for the integrals appearing in Eq. (10) and the matrix elements of $[\mathbf{A}]$ [28]. However, singularities occur when $\mathbf{r} = \mathbf{r}'$. The singularity problem is usually solved by estimating the Bessel functions in the limit of small $\mathbf{r} = \mathbf{r}'$, which results in integrable functions. However, to avoid this difficulty we utilized the analytical integration results developed by Ang [53]. Here the integral over any element, including the singular elements, can be computed without resorting to the more expensive Gaussian quadrature or similar numerical integration schemes.

Using the mass conservation principle for the step element we can calculate the relationship between flux, concentration, and velocity as

$$D\frac{\partial c}{\partial x} = v_x(c - c_s), \tag{12}$$

where x is perpendicular to the step element and c_s is the concentration in the solid. After scaling x with the step height h and using the dimensionless concentration in an equilibrium condition we have

$$\left.\frac{\partial u}{\partial n'}\right|_{\text{step}} = p_x\left(1 - \frac{1}{\Delta}\right) - p_x u, \tag{13}$$

where $\frac{\partial u}{\partial n'}|_{\text{step}}$ is the flux at the step and $\Delta = \frac{c_e - c_0}{c_e - c_s}$ is the supersaturation. Therefore, since scaled concentration is unity under equilibrium conditions, $\frac{\partial u}{\partial n'}|_{\text{step}} = -\frac{p_x}{\Delta}$ represents the linear relationship between supersaturation and Péclet number under the assumption of local equilibrium at the step face.

III. RESULTS AND DISCUSSIONS

Figure 1 shows the geometry of the domain we consider in this study. The interface consists of a series of steps of uniform height as well as terraces, which is the characteristic geometry of the ledge mechanism. Figure 1 is a snapshot from a molecular dynamics simulation [54] of pure Si (the red atoms) solidifying into an Al-Si liquid. The faceted interface is a vicinal 111 boundary.

In this study we assumed that steps are equally spaced. Therefore a domain whose bottom boundary includes a single step and has a length equal to the half distance of neighboring terraces can represent the whole system. The computational domain in the vertical direction extends up to the length (δ). By setting the scaled concentration to zero all along the top boundary we are assuming that there exists a boundary layer of dimension δ after which convective mixing fixes the liquid composition at its average value. Clearly, the effect of convection limits the solution to solid-liquid or solid-vapor systems, and the stagnant case, valid for alloys, will be treated in a subsequent section. Since the height of the step is on the order of atomic height, we assume the concentration along the step is constant and the step is in equilibrium ($u = 1$). In the previous conformal mapping solution by Jones and Trivedi the concentration along the step varies considerably, and an advantage of the BEM is the ability to maintain a fixed value of $u = 1$ along the step face.

To set the boundary conditions along the two sides of the computational domain we exploit the fact that the system is periodic in x. Therefore, we solve the Helmholtz equation

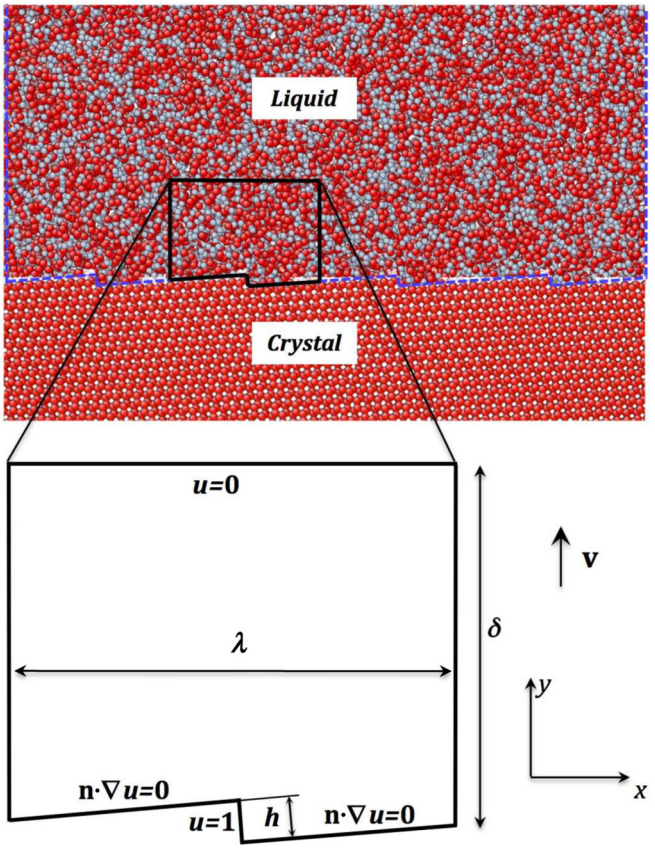

FIG. 1. (Color online) The geometry of the computational domain and the boundary conditions used in the boundary integral formulation. The periodicity in the x direction is given by λ, and the length along y is boundary layer thickness δ. The equilibrium concentration is assumed along the step face, and a zero flux condition is applied at the immobile terraces.

subject to the following:

$$u\left(-\frac{\lambda}{2},y\right) = u\left(\frac{\lambda}{2},y\right),$$
$$\left.\frac{\partial u}{\partial n'}\right|_{x=-\frac{\lambda}{2}} = -\left.\frac{\partial u}{\partial n'}\right|_{x=\frac{\lambda}{2}}. \quad (14)$$

Here we must distinguish the actual step spacing λ with the x dimension of the computational domain, which has been denoted by T. A simple geometric expression relates the two quantities: $\lambda = T\cos\theta + \frac{h}{2}\sin\theta$ where θ is the angle between the terrace and periodicity direction. There are several different ways to apply the above boundary condition in a boundary integral code. We followed the method explained in detail in Ref. [53], which requires the addition of two sets of unknowns, rather than one, for each element at the sides of the domain, and at the same time two sets of constraint equations based on periodic boundary conditions given above.

In the following results all elements were the same length, set equal to the length of the step face. Thus, the total number of nodes is in proportion to the terrace length and δ. That is, $T/h+1$ and T/h along the bottom and the top boundaries of the domain, respectively, and δ/h on the two vertical sides.

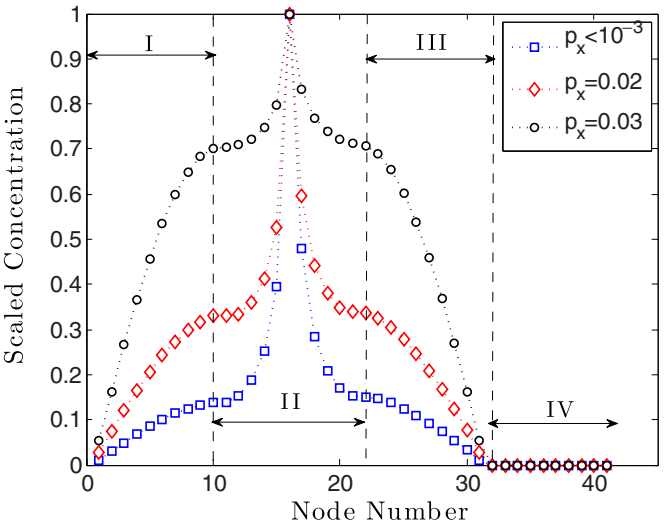

FIG. 2. (Color online) Concentration profile along the four boundaries for a system with dimensions $T = 10h$ and $\delta = 10h$. The position of the step is the center of domain II.

As mentioned above, all integrals in the BEM procedure were evaluated analytically.

The value of the Péclet number for solidification where the diffusion coefficient in liquid phase is on the order of $10^{-5}\frac{\text{cm}^2}{s}$ and for a system like Al-Si, with step height of $h = 3.15\times10^{-8}$ cm, would be on the order of 10^{-6}. Therefore the velocity of the step is negligible when compared with the bulk diffusion flux, and the term including Péclet number in Eq. (2) could be ignored. Thus, the Helmholtz equation reduces to the Laplace equation. The equivalent boundary condition would be zero flux for side boundaries, which is similar to the boundary condition used in other studies [2,29]. The range of validity of the Laplace equation assumption will be investigated below.

The scaled concentration and flux along the boundary of the domain are shown in Figs. 2 and 3, respectively, for a domain with terrace length of $T = 10h$ and diffusion length

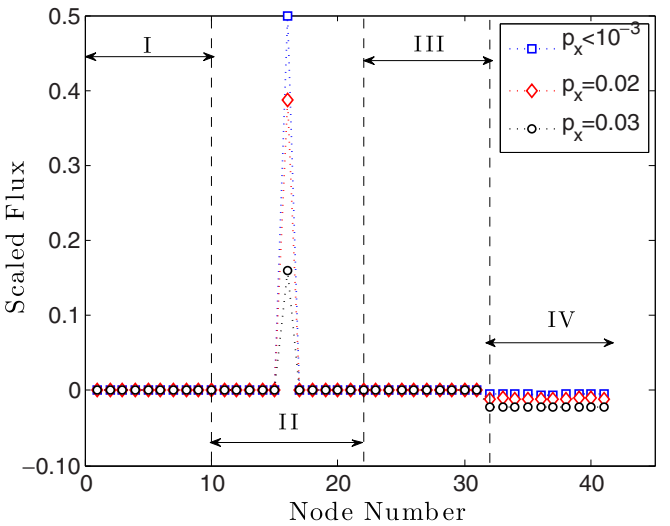

FIG. 3. (Color online) Flux across for all boundary nodes boundary for a system characterized by $T = 10h$ and $\delta = 10h$.

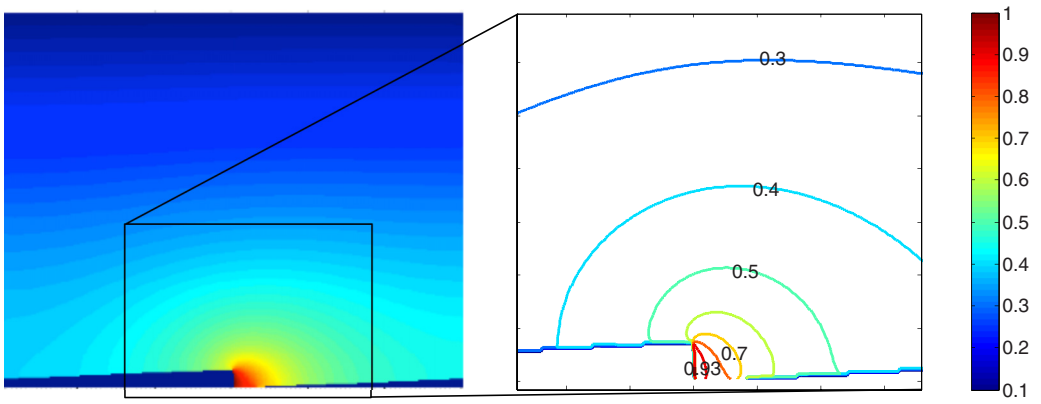

FIG. 4. (Color online) Concentration profile for an isolated step with $p_x = 10^{-3}$. The dimension of the domain are $T = 10h$, $\delta = 80h$.

of $\delta = 10h$. A range of Péclet numbers are summarized in the plots.

The origin of the domain is the upper left corner; therefore regions (**I**) to (**IV**) represent the left, bottom, right, and top sides of the domain, respectively. Therefore, region (**II**) includes two half size terraces and the step. We can observe a nearly linear variation of concentration along the side edges, from zero to a value between zero and unity. However, the concentration profile along terraces is neither linear nor symmetric. For Péclet numbers less than 10^{-3} the effect of velocity can be ignored. However, for higher Péclet numbers the concentration difference along the terraces decreases. Figure 3 shows that the flux along the left and right boundaries is almost zero, and across the step the flux decreases for higher Péclet numbers.

Figure 4 shows the concentration profile in the liquid surrounding the step where $T = 10h$, $\delta = 80h$, and $p_x = 10^{-3}$.

In these results we can see the asymmetry of the concentration profile with respect to the step. The asymmetry is a result of treating the step explicitly in the computation. In cases where the step is considered as a source point [2,29] the concentration field is radially symmetric about the step. In addition, a fast drop in concentration with increasing distance normal to the step is captured, and again we did not make the assumption of variable concentration along the step as was done in previous studies [31,33].

Figure 5 shows the concentration profile for a case where $T = 10h$ and $\delta = 50h$ and a Péclet number an order of magnitude more than that shown in Fig. 4, $p_x = 10^{-2}$. As expected, at higher velocities concentration profile is closer to equilibrium along the terraces. It should be noted that we ignored the solute trapping during transformation in this study and assumed that concentration along the step is in equilibrium. In addition, comparison between concentration isolines shows that asymmetry of the concentration profile increases by increasing the velocity.

As was shown in Eq. (13) we can define a relationship between Péclet number, supersaturation, and flux at the step where under the assumption of equilibrium concentration along the step face it simplifies to the relationship $\frac{\partial u}{\partial n'}|_{\text{step}} = -\frac{p_x}{\Delta}$. If the step velocity is sufficiently low and the dimensions of the domain are such that the Laplace equation is a good description of the concentration profile, then the derivative $\frac{\partial u}{\partial n'}|_{\text{step}}$ is a constant and a linear relationship is predicted between the Péclet number and the supersaturation. In the results of Figs. 6 and 7 the BEM-computed velocities are compared with this linear prediction.

In Fig. 6 we show the effect of terrace length on the relationship between supersaturation and scaled velocity. At a constant supersaturation, the scaled velocity is higher for larger step spacing. However, the effect of terrace length can be ignored when the terrace length is more than a critical value,

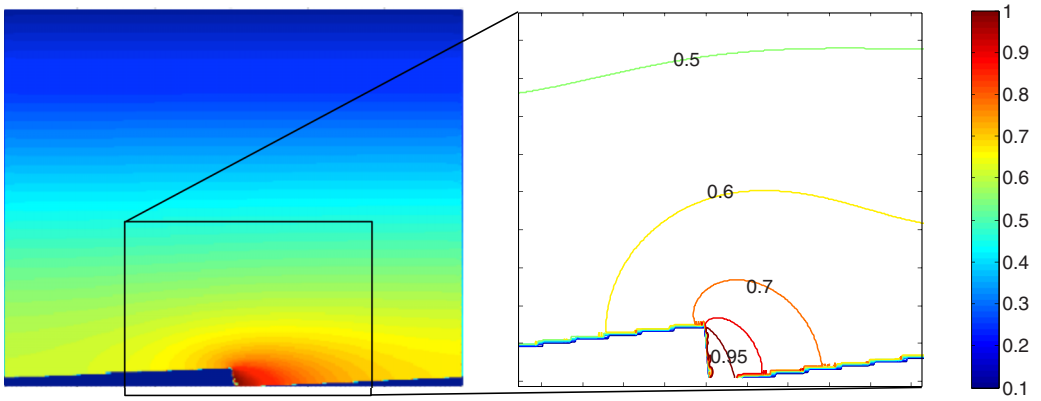

FIG. 5. (Color online) Concentration profile for an isolated step with $p_x = 10^{-2}$ ($T = 10h$ and $\delta = 50h$).

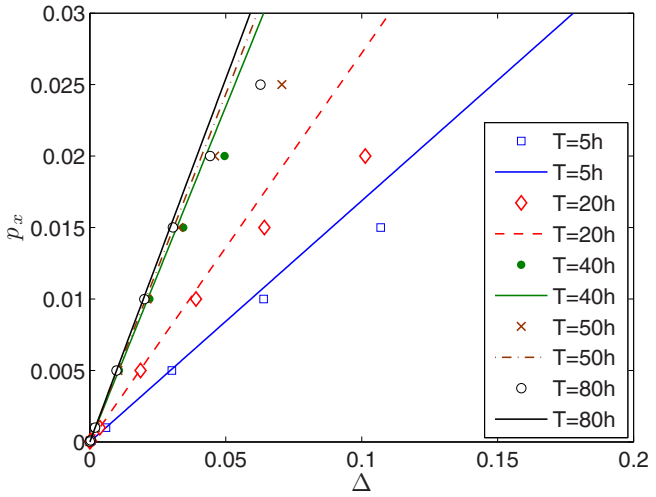

FIG. 6. (Color online) The Péclet number vs step spacing showing the effect of step separation on the kinetics of the transformation. The width of the boundary layer for all simulations is constant and equal to $50h$.

which is roughly $T = 40h$. However, this critical value is a function of boundary layer dimension, and for a system with longer δ this critical value increases. It is also evident from Fig. 6 that the linear relationship between step velocity and supersaturation is obeyed for small Δ but deviates sublinearly for higher Δ. The value of the supersaturation where the departure from linearly begins appears to decrease slightly with increasing step spacing.

The other geometric parameter affecting the relationship between scaled velocity and supersaturation is boundary layer width, the relationship of which is shown in Fig. 7. This figure suggests that for a certain supersaturation, the scaled velocity is higher for the systems with smaller layer widths. In addition, deviation from linearity occurs at lower Péclet numbers, for the systems with longer δ. For a system with a very small boundary

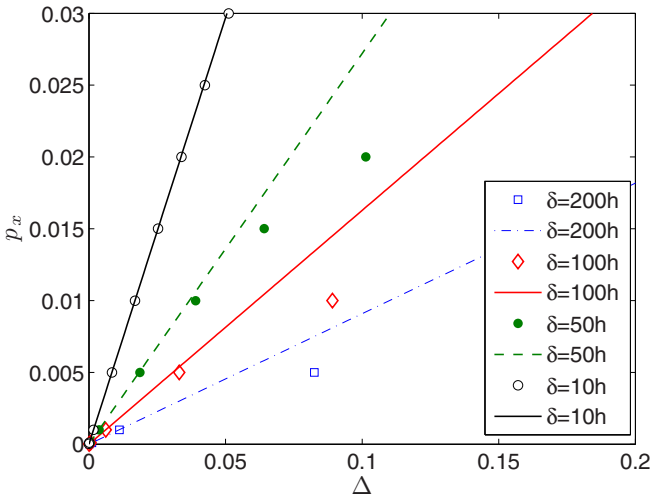

FIG. 7. (Color online) Effect of boundary layer size on the growth kinetics of transformation. Step separation for all simulations is constant and equal to $10h$.

layer, even at a Péclet number around 0.04, the linear relation between p_x and Δ is still valid.

IV. STEP BUNCHING

In this part we are use the technique and results we obtained in the previous section to test whether the step bunching phenomenon can occur in diffusion-controlled crystal growth. From experimental observations it has been suggested that equally spaced steps are inherently not stable and step trains tend to form bunches of steps close to each other, where each of these bunches are separated with a long terrace. It is interest to speculate as to the origin of step bunching in the case of diffusion-controlled growth from a condensed phase. As mentioned in the introduction the generally accepted mechanism of the step bunching instability in vapor growth systems is an asymmetry of the flux at each step. As shown in the concentration profiles in Figs. 4 and 5 the step geometry itself introduces a natural flux asymmetry, which we suggest is the underlying cause of the instability. It should be noted that the asymmetry is absent in the analytic solution in Ref. [29].

The problem of bunching in crystals is very important, since it is closely related to the problem of defect formation. A rigorous treatment of the step bunching problem would entail a linear stability of the equal step spacing geometry; that is, the step spacing is perturbed by an infinitesimally small amplitude perturbation with some prescribed wavelength. The change with time is then formulated, and if the amplitude increases with time the interface is unstable. However, since the base state of the problem cannot be solved analytically, the linear stability investigation is difficult. Therefore, in this study we will take a simplified approach which will yield the increase of flux to each step after a single step is repositioned by some amount along the interface. Although the procedure is not able to determine if the step array is linearly stable or not, it will show that perturbations of sufficient size can lead to step bunching.

The procedure adopted can be illustrated with reference to Fig. 8, which shows the central portion of three separate systems. The total number of steps in each computation is 25, the diffusion boundary length is taken as $\delta = 50h$, and all other boundary conditions are the same as described above. The top portion of Fig. 8 shows the step separation when all steps are equally spaced by $T = 8h$. The middle figure shows

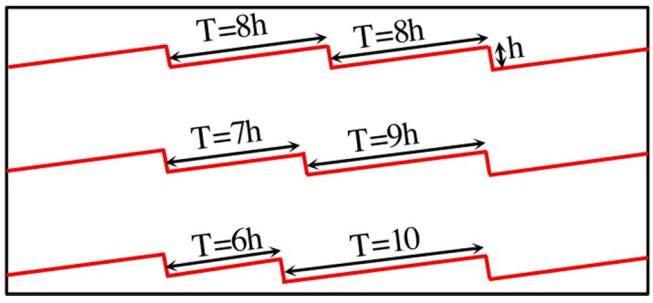

FIG. 8. (Color online) Geometry of the system in the vicinity of the central step. The top figure corresponds to no perturbation, whereas the middle and bottom figures correspond to perturbations of the central step equal to h and $2h$, respectively.

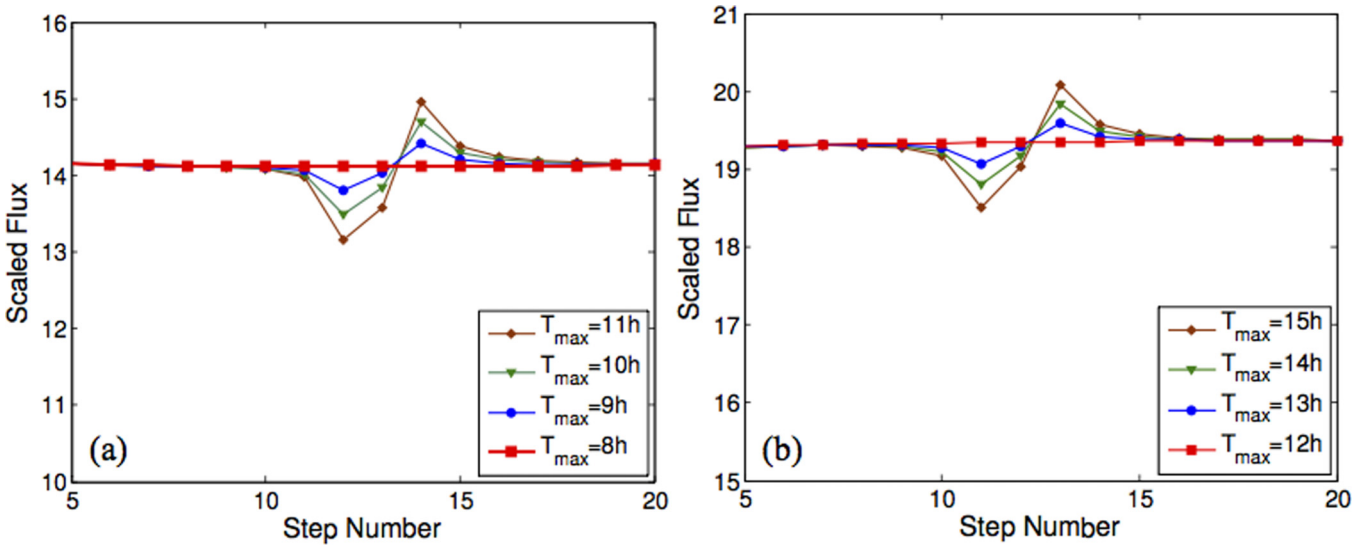

FIG. 9. (Color online) Scaled flux at each step at different terrace length perturbations for the systems with initial terrace lengths of (a) $8h$ and (b) $12h$. A boundary layer of $\delta = 50h$ was used for all computations.

a perturbation, equal to h, of the center step in the negative x direction, and the bottom figure shows the case of a $2h$ perturbation. In each case the BEM calculation provides the flux, and hence velocity, of each step. If the center step and those trailing it exhibit a velocity that is lower than the equally spaced case and the steps leading the center step show an increased velocity, then the interface is unstable with respect to step bunching.

Figure 9 shows the result of the analysis. The left plot corresponds to the case where the unperturbed system consists of steps spaced by $8h$, and the notation in the legend lists the length of the leading terrace used in each calculation. As expected the step velocity is equal for the equally spaced steps. However, the results clearly show a tendency to step bunching with the trailing steps slowing down and the leading steps speeding up after the perturbation is introduced. In this case the influence of the perturbation extends over roughly five steps to either side of the central step. Furthermore, as the perturbation increases in magnitude the effect is amplified, which implies the step bunching will grow after the initial perturbation. The right plot of Fig. 8 shows the same procedure for the case of an initial $12h$ spacing of steps. The qualitative trend is equivalent to $T = 8h$ result.

For a better comparison of the effect of a perturbation on step bunching behavior for different terrace lengths, we perform a series of BEM calculations in which the perturbation is kept fixed at 10% of total terrace length. In other words, for the system with terrace length of $10h$ the perturbation is h, and for the case of $T = 100h$ perturbation is $10h$. Furthermore, in order to accurately compare the change in step velocity in each computation, the flux at each sets is normalized by the baseline flux obtained from the case of equally spaced steps. As above, in each computation the total number of steps is 25 and $\delta = 50h$. The results are presented in Fig. 10, and the data show that for equal percentage of perturbation, the change in flux of steps is increased for smaller terrace lengths. The numerical results suggest that an interface with closely spaced steps is more susceptible to step bunching than interfaces with longer terraces. In the long wavelength limit, i.e., infinitely spaced steps, the interface appears to be neutrally stable. It is important to note that the computations presented here neglect any elastic interaction between steps, which will affect the equilibrium concentration at the step face [55]. It is expected that the inclusion of elastic energy will tend to stabilize the system for small wavelength perturbations (small step spacings).

V. ANALYTIC SOLUTION, STAGNANT CASE

As mentioned in the previous section, the assumption of a boundary layer implies convective mixing occurs in the liquid

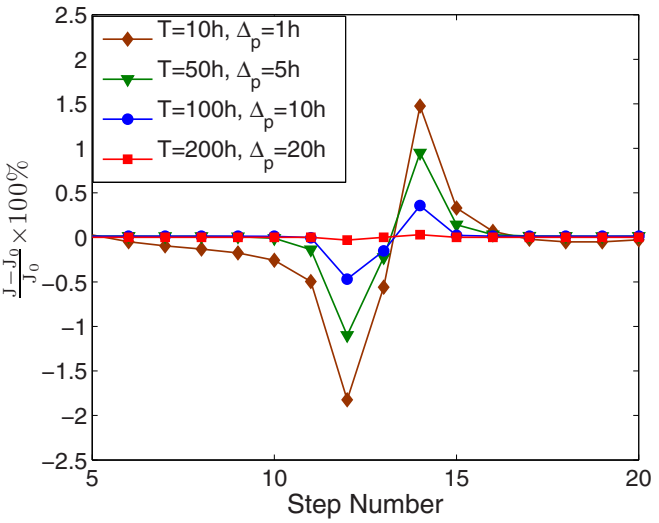

FIG. 10. (Color online) Comparison of the normalized step velocity for an equal percentage of perturbation (10%) at the terrace length range of $T = 10h$ to $T = 200h$. J is the scaled flux for a perturbed system, and J_0 is the scaled flux of steps in an equally spaced system.

phase. In this section we formulate an analytic solution to the diffusion-controlled growth of a step-terraced interface for the case of no convection. The solution will be applicable to the growth of stepped interfaces in solid-solid systems.

To proceed we note that as the boundary layer width δ increases, the concentration gradient at the step decreases linearly with the distance y, and eventually the growth rate will approach zero. However, in the computation we have neglected the velocity of the interface in the y direction. Inclusion of a v_y term, no matter how small, will guarantee a finite flux and growth rate in the limit $\delta \to \infty$ [56,57]. The above discussion implies that an approximate solution can be developed using a matched asymptotic expansion. A similar approach has been employed in Ref. [32].

Now we can consider the more complicated case where the velocity in any x or y direction cannot be ignored. Therefore the diffusion equation in the unscaled coordinates would be

$$D\nabla^2 u + v_x \frac{\partial u}{\partial x} + v_y \frac{\partial u}{\partial y} = 0. \tag{15}$$

To obtain an "outer" solution note that sufficiently far from the interface ($y \sim T$) all variations of u in the x direction become vanishingly small. The diffusion equation reduces to $\frac{\partial^2 u}{\partial y^2} + v_y \frac{\partial u}{\partial y} = 0$, and the outer solution is given by

$$u_{\text{out}}(\tilde{x},\tilde{y}) = A' \exp(-p_y \tilde{y}) + B', \tag{16}$$

where, anticipating the inner solution, we have rescaled all lengths by $\tilde{x} = x/h$, $\tilde{y} = y/h$, and $\tilde{\lambda} = \lambda/h$. In the above solution, the boundary condition $u(\tilde{x},\tilde{y} \to \infty) = 0$ forces B' to be zero.

To formulate the inner solution we identify a small parameter as h the step height and rescale all length variables in the diffusion equation. The result is simply $\nabla^2 u = 0$ where all terms of order of the Péclet number have been neglected. An approximate general solution to the Laplace equation for a periodic step train has been derived by Chernov using a conformal mapping procedure. Assuming a step spacing much larger than the step height, the general solution is given by

$$u_{\text{in}}(\tilde{x},\tilde{y}) = \frac{A}{2} \ln\left[\sin^2\left(\frac{\pi}{\tilde{\lambda}}\tilde{x}\right) + \sinh^2\left(\frac{\pi}{\tilde{\lambda}}\tilde{y}\right)\right] + B. \tag{17}$$

Chernov completed the problem by applying a kinetically limited boundary condition at the step. Here we apply a diffusion-controlled condition. Noting that the solution assumes the steps are represented by point sources of solute, we apply the boundary condition $u(1,0) = u(0,1) = 1$, which means, on the surface of a half cylinder surrounding the step with radius equal to the height of the step, the composition is equal to the equilibrium composition. Applying this boundary condition, the constant B can be obtained as

$$B = 1 - A \ln\left(\frac{\pi}{\tilde{\lambda}}\right). \tag{18}$$

So far we have determined the solution of the diffusion equation for the inner and the outer regions. However, there are two constants remaining in Eqs. (17) and (16). To complete the problem we apply a formal matching procedure, which is given by $u_{\text{out}}(\tilde{y} \to 0) = u_{\text{in}}(\tilde{y} \to \infty)$. For the inner region [Eq. (17)] the sin term can be neglected relative to the sinh term, and, using the definition of $\sinh\left(\frac{\pi}{\tilde{\lambda}}\tilde{y}\right) = \frac{\exp\left(\frac{\pi}{\tilde{\lambda}}\tilde{y}\right) - \exp\left(-\frac{\pi}{\tilde{\lambda}}\tilde{y}\right)}{2}$, the limits become

$$u_{\text{in}}(\tilde{x},\tilde{y}) = A\left[\left(\frac{\pi}{\tilde{\lambda}}\right)\tilde{y} - \ln\left(\frac{2\pi}{\tilde{\lambda}}\right)\right] + 1, \tag{19}$$

$$u_{\text{out}}(\tilde{x},\tilde{y}) = A'\left(1 - p_y \tilde{y}\right). \tag{20}$$

A solution for the concentration field, valid over the entire domain, can be obtained via $u(\tilde{x},\tilde{y}) = u_{\text{in}} + u_{\text{out}} - u_{\text{match}}$, where u_{match} is the value of the field under the matching procedure. Therefore the final result reads

$$u(\tilde{x},\tilde{y}) = \frac{A}{2} \ln\left[\sin^2\left(\frac{\pi}{\tilde{\lambda}}\tilde{x}\right) + \sinh^2\left(\frac{\pi}{\tilde{\lambda}}\tilde{y}\right)\right] + B + A' \exp(-p_y \tilde{y}) - A'(1 - p_y \tilde{y}), \tag{21}$$

where $A = -\frac{p_y \tilde{\lambda}}{\pi - p_y \tilde{\lambda} \ln\left(\frac{2\pi}{\tilde{\lambda}}\right)}$, $A' = \frac{\pi}{\pi - p_y \tilde{\lambda} \ln\left(\frac{2\pi}{\tilde{\lambda}}\right)}$ and B is determined based on Eq. (18).

The concentration profile resulting from Eq. (21) for $\tilde{x} = 0$, which represents the profile from the step into the liquid, is shown in Fig. 11. Notice that the inner solution decreases linearly and without bound as $\tilde{y}$ tends to infinity, whereas the matched asymptotic solution exhibits the correct exponential decay for large $\tilde{y}$.

Our ultimate goal is to determine the growth rate from the analytic solution to the concentration field. Recall the step is treated as a semicircle with radius equal to the step height. Thus, for calculation of the flux it is easier to transform Eq. (21) to cylindrical coordinates, which is given by

$$u(r,\phi) = \frac{A}{2} \ln\left[\sin^2\left(\frac{\pi}{\tilde{\lambda}} r\cos\phi\right) + \sinh^2\left(\frac{\pi}{\tilde{\lambda}} r\sin\phi\right)\right] + B + A' \exp(-p_y r\sin\phi) - A'(1 - p_y r\sin\phi). \tag{22}$$

For sufficiently small r, that is, in the vicinity of the step, the next to last term can be expanded in a Taylor series and, when combined with the last term, leads to a contribution of order p_y^2, which will be neglected. With this simplification, the concentration does not vary with ϕ in the region near the step. In other words, $\frac{\partial u}{\partial \phi}|_{r\to 1} = 0$. In addition, the gradient of the concentration in the radial direction is equal at all angles including $\phi = \frac{\pi}{2}$. Using these assumptions we obtain

$$\left.\frac{\partial u}{\partial r}\right|_{r=1,\ \text{any}\ \phi} = \left.\frac{\partial u}{\partial r}\right|_{r=1,\ \phi=\frac{\pi}{2}} = \frac{A\pi}{\tilde{\lambda}}\left[\frac{\cosh\left(\frac{\pi}{\tilde{\lambda}}\right)}{\sinh\left(\frac{\pi}{\tilde{\lambda}}\right)}\right] - A' p_y [\exp(-p_y) + 1]. \tag{23}$$

Applying the mass conservation principle, the flux into the inner semicircle with the area of πh, is equal to the flux at the step with height of h. In scaled coordinates, $\pi \frac{\partial u}{\partial r} = \frac{\partial u}{\partial n'}$. Combining Eqs. (13) and (23) and noting that $u = 1$ at the step, the step velocity is then given by

$$p_x = \frac{\pi \Delta \tilde{\lambda}}{2\pi^2 \Delta - \tilde{\lambda}\pi \ln\left(\frac{2\pi}{\tilde{\lambda}}\right)}, \tag{24}$$

where the p_y term appearing in the constant A was converted using $p_y = p_x \sin(h/\lambda) \approx p_x/\tilde{\lambda}$. Also, the terms involving the

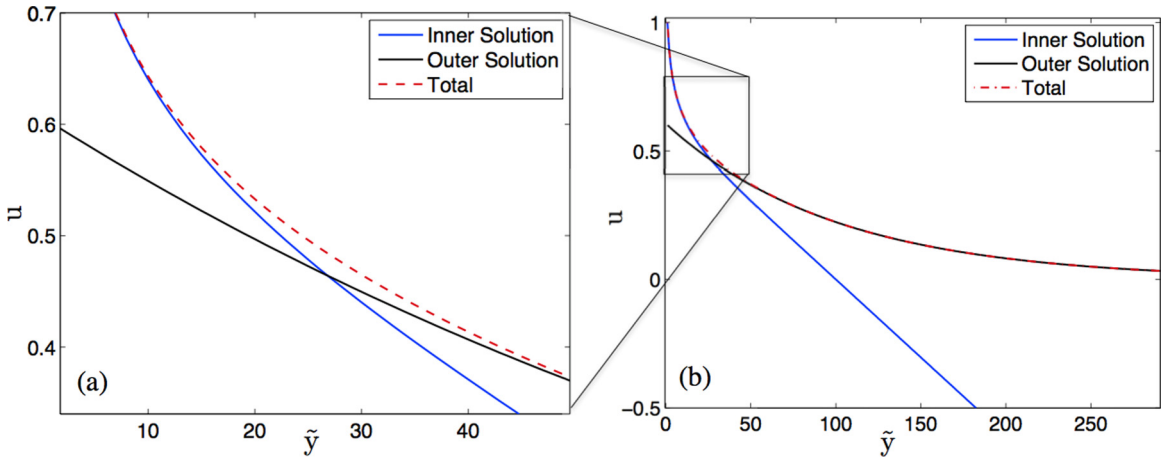

FIG. 11. (Color online) Results of the matched asymptotic analysis showing the inner and outer regions and the final composition profile. The profile is shown as a function of $\tilde{y}$ and $\tilde{x}$ is set equal to the step position, i.e., $\tilde{x} = 0$.

hyperbolic functions were simplified under the assumption of large $\tilde{\lambda}$.

The above approximate result predicts that the step velocity in the x direction decays to zero as the interstep spacing $\tilde{\lambda}$ increases. Unfortunately, this behavior contrasts with the analytic results obtained by Jones and Trivedi and Atkinson for the case of an isolated step. However, the decrease in p_x with spacing predicted by the above result is characterized by a slowly varying logarithmic dependence. Figure 12 shows the scaled velocity versus supersaturation for different step spacing values computed using Eq. (24). Based on this model, for a specific supersaturation, the step velocity is higher for a smaller step spacing. The variation with $\tilde{\lambda}$ is large for step spacings that are relatively small, as is evident from the curves labeled $\tilde{\lambda} = 10$ to 50. For larger spacings the variation is much slower with a small difference observed for the order of magnitude change from $\tilde{\lambda} = 100$ to 1000. For comparison the Jones and Trivedi result is shown by the open circles, and the two results compare favorably in the vicinity of $\tilde{\lambda} = 100$.

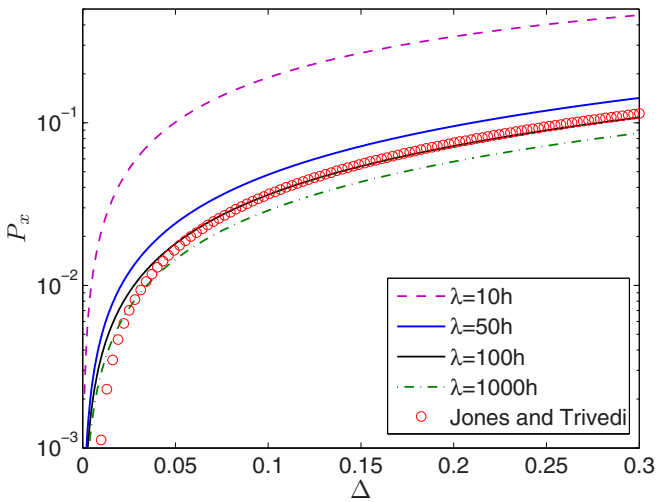

FIG. 12. (Color online) Scaled velocity of the step vs supersaturation for different λ. The results of Ref. [31] are compared with the calculation of the present study.

VI. CONCLUSION

The boundary element method has been used to compute the growth rate and concentration profile for the case of an infinite and periodic array of mobile interface steps separated by immobile terraces. An important assumption in the numerical study is the existence of a boundary layer at the interface, beyond which there exists complete mixing in the fluid. The BEM results therefore describe the case of vicinal surfaces growing into a liquid or vapor. Growth rates have been computed as a function of two important variables: the step spacing and the boundary width. The computations indicate that the step velocity varies linearly with supersaturation for low supersaturation and deviates below linear at high Δ. The departure from linear behavior occurs at lower supersaturation for increasing boundary layer width. The BEM computations were also used to study the effect of geometry of the system on the tendency for step bunching. We have investigated the special case where the position of one central step is perturbed. It was concluded that the equally spaced steps are not stable to sufficiently large perturbations, and the system tends to form separated bunches of steps.

For the case of a stagnant liquid or a step-terraced interface separating two crystalline phases, an approximate analytic solution has been derived. The solution is based on a matched asymptotic expansion technique, and the solution valid in the vicinity of the step is formulated from a conformal mapping procedure. The results predict that for a given supersaturation the step velocity decreases with increasing step spacing.

ACKNOWLEDGMENTS

The authors would like to thank Mary Gallerneault for her contribution in the proofreading and editing of this paper.

[1] J. Frenkel, *Kinetic Theory of Liquids* (Clarendon Press, Oxford, 1946).

[2] W. K. Burton, N. Cabrera, and F. C. Frank, The growth of crystals and the equilibrium structure of their surfaces, Phil. Trans. R. Soc. Lond. A **243**, 299 (1951).

[3] M. S. o. A. F. M. Committee, *Decomposition of Austenite by Diffusional Processes: Proceedings of a Symposium Held in Philadelphia, Pennsylvania, October 19, 1960 under the Sponsorship of the Ferrous Metallurgy Committee of the Institute of Metals Division, the Metallurgical Society, American Institute of Mining, Metallurgical, and Petroleum Engineers* (Interscience Publishers, New York, 1962).

[4] G. Binnig and H. Rohrer, Scanning tunneling microscopy from birth to adolescence, Rev. Mod. Phys. **59**, 615 (1987).

[5] Y.-W. Mo, R. Kariotis, B. S. Swartzentruber, M. B. Webb, and M. G. Lagally, Scanning tunneling microscopy study of diffusion, growth, and coarsening of Si on Si(001), J. Vac. Sci. Technol. A **8**, 201 (1990).

[6] G. J. Shiflet, Growth by ledges, Interface Sci. **6**, 133 (1998).

[7] H. I. Aaronson, On the mechanism of formation of diffusional plate-shaped transformation products, Acta Mater. **54**, 1227 (2006).

[8] S. A. Hackney, The pearlite-austenite growth interface in an Fe-0.8 C-12 mn alloy, Acta Metall. **35**, 1007 (1987).

[9] K. Campbell, The isothermal decomposition of austenite in simple chromium steels, Metal Sci. **8**, 197 (1974).

[10] P. Merle and J. Merlin, Coarsening of plates in Al-Cu alloys. II. Influence of ledge mechanism, Acta Metall. **29**, 1929 (1981).

[11] J. M. Howe, Atomic mechanisms of precipitate plate growth in the Al–Ag system. II. High-resolution transmission electron microscopy, Acta Metall. **33**, 649 (1985).

[12] J. M. Howe, Atomic mechanisms of precipitate plate growth in the Al–Ag system. I. Conventional transmission electron microscopy, Acta Metall. **33**, 639 (1985).

[13] J. M. Howe, Atomic mechanisms of precipitate plate growth, Philos. Mag. **56**, 31 (1987).

[14] U. Dahmen and K. H. Westmacott, Ledge structure and the mechanism of precipitate growth in Al–Cu, Phys. Status Solidi A **80**, 249 (1983).

[15] S. A. Hackney, Interfacial structure of Θ precipitates in Al-5 wt.% Cu alloys, Mater. Sci. Eng. A **113**, 153 (1989).

[16] W. Cassada, Mechanism of Al_2CuLi (T_1) nucleation and growth, Metall. Trans. A **22**, 287 (1991).

[17] Z.-W. Cui, F. Gao, and J.-M. Qu, On the perturbation solution of interface-reaction controlled diffusion in solids, Acta Mech. Sinica **28**, 1049 (2012).

[18] J.-Y. Go and S.-I. Pyun, A review of anomalous diffusion phenomena at fractal interface for diffusion-controlled and non-diffusion-controlled transfer processes, J. Solid State Electrochem. **11**, 323 (2007).

[19] Y. C. Liu, F. Sommer, and E. J. Mittemeijer, The austenite ferrite transformation of ultralow-carbon Fe-C alloy; transition from diffusion- to interface-controlled growth, Acta Mater. **54**, 3383 (2006).

[20] W. W. Mullins and R. F. Sekerka, Stability of a planar interface during solidification of a dilute binary alloy, J. Appl. Phys. **35**, 444 (1964).

[21] D. J. Wollkind and L. A. Segel, A nonlinear stability analysis of the freezing of a dilute binary alloy, Phil. Trans. R. Soc. Lond. A **268**, 351 (1970).

[22] G. Horvay and J. W. Cahn, Dendritic and spheroidal growth, Acta Metall. **9**, 695 (1961).

[23] W. P. Bosze and R. Trivedi, The effects of crystallographic anisotropy on the growth kinetics of Widmanstätten precipitates, Acta Metall. **23**, 713 (1975).

[24] W. P. Bosze and R. Trivedi, On the kinetic expression for the growth of precipitate plates, Metall. Trans. **5**, 511 (1974).

[25] D. Quidort and Y. J. M. Brechet, Isothermal growth kinetics of bainite in 0.5% C steels, Acta Mater. **49**, 4161 (2001).

[26] Z. Guo and W. Sha, Kinetics of ferrite to Widmansättten austenite transformation in a high-strength low-alloy steel revisited, Z. Metallkd. **95**, 718 (2004).

[27] M. Hillert, L. Höglund, and J. Ågren, Diffusion-controlled lengthening of Widmansättten plates, Acta Mater. **51**, 2089 (2003).

[28] J. J. Hoyt, The velocity of plate precipitates growing by the ledge mechanism, Acta Mater. **61**, 4953 (2013).

[29] A. A. Chernov, The spiral growth of crystals, Sov. Phys. Usp. **4**, 116 (1961).

[30] M. Ohara and R. C. Reid, *Modeling Crystal Growth Rates from Solution* (Prentice-Hall, New York, 1973).

[31] G. J. Jones and R. K. Trivedi, Lateral growth in solid-solid phase transformations, J. Appl. Phys. **42**, 4299 (1971).

[32] C. Atkinson, The growth kinetics of individual ledges during solid-solid phase transformations, Proc. R. Soc. Lond. A **378**, 351 (1981).

[33] C. Atkinson, The growth kinetics of ledges during phase transformations: multistep interactions, Proc. R. Soc. Lond. A **384**, 107 (1982).

[34] C. Atkinson, Diffusion controlled ledge growth in a medium of finite extent, J. Appl. Phys. **53**, 5689 (1982).

[35] M. Enomoto, Computer modeling of the growth kinetics of ledged interphase boundaries. I. Single step and infinite train of steps, Acta Metall. **35**, 935 (1987).

[36] M. Enomoto, Computer modeling of the growth kinetics of ledged interphase boundaries. II. Finite train of steps, Acta Metall. **35**, 947 (1987).

[37] M. Enomoto, Computer simulation of morphological changes of grain boundary precipitates growing by the ledge mechanism, Metall. Trans. A **22**, 1235 (1991).

[38] M. Enomoto and C. Atkinson, Diffusion-controlled growth of disordered interphase boundaries in finite matrix, Acta Metall. Mater. **41**, 3237 (1993).

[39] G. Spanos, R. A. Masumura, R. A. Vandermeer, and M. Enomoto, The evolution and growth kinetics of precipitate plates growing by the ledge mechanism, Acta Metall. Mater. **42**, 4165 (1994).

[40] A. A. Chernov, Crystal growth science between the centuries, J. Mater. Sci.: Mater. Electron. **12**, 437 (2001).

[41] F. C. Frank, in *Growth and Perfection of Crystals*, edited by R. Dormus, B. Roberts, and D. Turnball (Wiley, New York, 1958).

[42] C. Duport, P. Nozières, and J. Villain, New instability in molecular beam epitaxy, Phys. Rev. Lett. **74**, 134 (1995).

[43] G. Ehrlich and F. G. Hudda, Atomic view of surface self-diffusion: tungsten on tungsten, J. Chem. Phys. **44**, 1039 (1966).

[44] R. L. Schwoebel, Step motion on crystal surfaces. II, J. Appl. Phys. **40**, 614 (1969).

[45] V. I. Bredikhin, G. L. Galushkina, A. A. Kulagin, S. P. Kuznetsov, and O. A. Malshakova, Competing growth centers

and step bunching in KDP crystal growth from solutions, J. Cryst. Growth **259**, 309 (2003).

[46] V. I. Bredikhin and O. A. Malshakova, Step bunching in crystal growth from solutions: model of nonstationary diffusion layer, numerical simulation, J. Cryst. Growth **303**, 74 (2007).

[47] V. I. Bredikhin, Mass-transport and step bunching in crystal growth from solutions, Transport Theor. Stat. Phys. **37**, 504 (2008).

[48] V. I. Bredikhin, O. A. Malshakova, and A. D. Yunakovsky, Traveling waves of step density and solution supersaturation in the assigned diffusion layer thickness model of step bunching, J. Cryst. Growth **312**, 1443 (2010).

[49] B. Q. Li, Boundary element solution of heat convection-diffusion problems, J. Comput. Phys. **93**, 255 (1991).

[50] D. I. Meiron, Selection of steady states in the two-dimensional symmetric model of dendritic growth, Phys. Rev. A **33**, 2704 (1986).

[51] Z. H. Qiu, L. C. Wrobel, and H. Power, Numerical solution of convection-diffusion problems at high Péclet number using boundary elements, Int. J. Num. Methods Eng. **41**, 899 (1998).

[52] C. A. Brebbia, J. C. F. Telles, and L. C. Wrobel, *Boundary Element Techniques* (Springer-Verlag, Berlin, 1984).

[53] W. T. Ang, *A Beginner's Course in Boundary Element Methods* (Universal Publishers, Boca Raton, FL, 2007).

[54] P. Saidi and J. J. Hoyt, Kinetic coefficient of steps at the Al-Si(111) crystal-melt interface from molecular dynamics simulations (unpublished).

[55] J. Tersoff, Y. H. Phang, Z. Zhang, and M. G. Lagally, Step-bunching instability of cicinal surfaces under stress, Phys. Rev. Lett. **75**, 2730 (1995).

[56] C. C. Lin and L. A. Segel, *Mathematics Applied to Deterministic Problems in the Natural Sciences* (Macmillan, New York, 1988).

[57] C. M. Bender and S. A. Orszag, *Advanced Mathematical Methods for Scientists and Engineers* (McGraw-Hill, New York, 1978).